Journal Homepage: http://ijcpe.uobaghdad.edu.iq
Iraqi Journal of Chemical and Petroleum Engineering
Vol. 27 No. 1 (March 2026) 127 – 142
EISSN: 2618-0707, PISSN: 1997-4884

Optimization and adsorption modeling of lead ions (II) on carbonaceous materials: Comparative evaluation of raw and citric acid-modified commercial activated carbon and tea waste derived biochar

Shaymaa H. Khazaal [a, *]

a Department of Applied Chemistry, College of Applied Sciences, University of Technology, Baghdad, Iraq

Abstract

The article investigated the effectiveness of removal (R%) of a batch study in the removal of lead (II) ions from synthetic aqueous water. A number of experiments were performed to determine the optimal parameters for the maximum removal procedure by using commercial activated carbon. The primary process variables studied included initial lead (II) ions concentration (pb (II)), pH, adsorbent particle size, dosage of adsorbent, and adsorption time.

The maximum removal occurred at an initial pb (II) ions concentration of 10 ppm, a pH of 5, an adsorbent dosage of 0.3 g with a particle size of 75 µm, and an adsorption time of 75 min. This research employed isotherm models to determine how the system reached a stable state. Langmuir model confirmed the largest accuracy, as evidenced by the results with a correlation coefficient (R^2) of about 97.91%. The kinetic data was the most accurately described by pseudo-second-order model (PSO), suggesting that chemisorption is the limiting factor in the reaction rate, which was supported by a correlation coefficient of 99.5%. Four different adsorbent materials were investigated to evaluate their lead ions (II) removal %: commercial activated carbon (CAC), tea waste-derived biochar (TWDB), and CAC and TWDB modified with citric acid (CAC-CA and TWDB-CA). The study demonstrated that these four adsorbents were very effective and inexpensive agricultural waste may serve as an efficient method to remove pb (II) ions from contaminant water.

Keywords: Lead Ions (II) Removal; Adsorption; Commercial Activated Carbon; Isotherms and kinetics; Tea Waste Derived Biochar; Citric Acid Modification.

Received on 09/02/2026, Received in Revised Form on 12/03/2026, Accepted on 14/03/2026, Published on 30/03/2026

https://doi.org/10.31699/IJCPE.2026.1.11

1- Introduction

The rising issues of heavy metals contamination in different aqueous environments represent an important global challenge to public health and environmental sustainability. Pb (II) ions is considered one of the most hazardous heavy metals, due to its high toxicity, non-biodegradability, and tendency to bioaccumulate in the living organisms [1, 2], posing very severe risks to eco-systems and human's health even at very tiny concentrations. The World Health Organization (WHO) have established stringent maximum permissible limits for pb in the drinking water at about 10-15 µg/L [3-5].

Various techniques have been working for the removal of heavy metals from wastewater, including chemical precipitation, electrochemical reduction, ion exchange, liquid membrane separation, cementation, and solvent extraction. However, the number of these techniques is limited by high costs, incomplete removal, and the generation of secondary toxic materials [6]. In this context, adsorption has emerged as a highly preferred technique due to its operational simplicity, high efficiency, cost effectiveness, and the ability for adsorbent regeneration [7].

Among the established removal methodologies, adsorption has been reported to be the most suitable process for its application feasibility and higher efficiency compared to other alternative technologies. The commonly used commercial adsorbents include zeolites, activated alumina, commercial activated carbon, silica gel, and synthetic polymers. In the last recent years, nanoparticles and carbon nanotubes (CNTs) have been used as adsorbents for removing heavy metals from wastewater, with the greater pore diameter and pore volume of nanoparticles and carbon nanotubes increasing their adsorption capacity [8, 9]. However, most of commercial and CNT-based adsorbents are very expensive, and the regeneration of these adsorbents materials is often not feasible, limiting their widespread application [4, 10].

Whereas CAC is the most widely utilized adsorbent according to its high surface area and developed porosity, its common application is often constrained by its

*Corresponding Author: Email: Shaymaa.H.AlKhasraji@uotechnology.edu.iq

relatively high cost and the energy intensive processes required for its regeneration and production [11, 12]. This economic obstacle has catalyzed an example shift in research towards the development of low cost; sustainable material adsorbents derived from an abundant and a renewable resource. According to a universal review by many researchers Chowdhury et al. [4], low cost material adsorbents can be characterized into different five groups: natural materials, industrial byproducts, agricultural waste, forest waste, and biotechnology based adsorbents materials, with adsorption equilibrium capacities ranged from about 0.8 - 333 mg/g for natural materials, 2.5 - 524 mg/g for industrial byproducts, and 0.7 - 2079 mg/g for agricultural waste materials, achieving R % between 13.6 – 100 %.

An agricultural waste and biomass byproduct has garnered considerable attention as promising precursors for CAC and producing biochar [13, 14]. These adsorbents are not only economically feasible but also contribute to a circular economy by valorizing waste streams. Biochar, a carbonic material produced from the partial combustion of biomass waste materials, has been labelled as black gold for its potential in water pollution mitigation and carbon sequestration. The recent studies demonstrate that biochar can achieve more than 90 % removal efficiency for heavy metals such as lead and cadmium, more than 85% adsorption capacity for organic pollutants such as phenols and dyes, and more than 80 % reduction in micro-plastics and nano-plastics [15]. A number of recent studies have investigated the significant potential of adsorbents for instance tea-waste, a widely available byproduct from the beverage industry, for the effective removal of different types of heavy metals from pollutant water. Dhobi et al., [16] investigated the efficiency of tea-derived absorbents and reported maximum removal of 97.7 % for nickel, 82 % for cadmium, 52.6 % for zinc, and demonstrating the selective adsorption behaviour and superior performance of tea-derived materials. Moreover, Rajput et al. developed a zerovalent iron-decorated tea waste-derived biochar composite that exhibited excellent removal performance for chromium and many organic dyes, prominence the versatility of tea-waste valorization [17].

To further enhancement the adsorption capacity and selectivity of these carbonic adsorbent's materials, chemical modification techniques are being intensively discovered. The functionalization of adsorbents surface with specific active chemical groups can significantly improve their attraction for targeted pollutants. Modification with organic acids, such as citric acid (CA), has proven to be a particularly effective technique. This process introduces carboxyl functional groups (‑COOH) onto the surface of adsorbent, which act as active binding sites for cationic heavy metals like lead through mechanisms such as surface complexation and ion exchange.

Liu et al., [18] investigated that citrate-modified biochar revealed substantially enhanced removal capacity for different types of heavy metals simultaneously, with the modification process transitioning the primary removal mechanism from physical adsorption to stronger chemical adsorption. Similarly, Ekanayake et al., [19] displayed that CA modification of derived biochar from plant biomass significantly enhanced the adsorption of chromium, providing evidence that organic acid functionalization is a viable strategy for enhancing adsorbent performance. Lach et al., [7] conducted a detailed analysis of cadmium and lead adsorption on commercial activated carbon, demonstrating that kinetic data were best fitted by PSO model, indicating that chemisorption was the rate-limiting step. Haider et al., [20] found that the pseudo-first-order (PFO) kinetic model introduced the most suitable for pb (II) ions removal on press mud based on R^2 and other goodness of fit measures, forecasting the physical adsorption of leaf, in which the rate of adsorption is directly related to the number of available active sites on the adsorbent surface, this work also proved that the biosorption of pb (II) ions increased with rising amount of adsorbent dosage from 2 - 10 g/L, which could be attributed to the increased availability of active sites, and that temperature significantly influenced adsorption, and with optimal adsorption happening at 37 °C. The intraparticle diffusion kinetics model has been identified as the best fit for describing the rate-limiting step in some systems, suggesting that the pore diffusion is the controlling mechanism in the interaction between pb (II) ions and the adsorption active site.

This work concerns the uptake of pb (II) ions in aqueous solution by CAC. In order to give a complete description of a batch adsorption system, experimental runs have been performed at different pb (II) ions concentrations, pH, adsorbent dosage, adsorbent particle size, adsorption time, and shaking rate. Tests identified optimal conditions. The isotherm and kinetic models were performed. Additionally, it assessed the effectiveness of pb (II) removal % utilizing four adsorbents (CAC, CAC-CA, TWDB, and TWDB-CA) at optimal conditions. The experiments systematically compare CAC with TWDB, including citric acid modification, under optimal conditions for the removal of Pb (II) ions. This study assesses performance, adsorption processes, and economic modification options within a cohesive experimental framework, in contrast to prior research that concentrates on a singular adsorbent.

2- Materials and methods

2.1. Chemicals

The chemicals utilized in this study, including lead nitrate (Pb $(NO_3)_2$), hydrochloric acid (HCl) 37 %, sodium hydroxide (NaOH), citric acid ($C_6H_8O_7$) with purity 99.5 %.

2.2. Adsorbents preparation

2.2.1. Commercial activated carbon (CAC)

Commercial activated carbon was collected from local chemical supplier and utilized in this study to investigate the optimal variables, which was dried at 200 °C,

thereafter ground, and sieved using an equipment from the chemical engineering department into three distinct particle size ranges: ≥ 75 µm, (75-100) µm, and (100-125) µm. BET surface area was 1,245.7 m^2/g.

2.2.2. Tea waste derived biochar (TWDB)

The adsorbent obtained from tea waste, referred to as tea waste-derived biochar (TWDB), was produced by methodically cleaning the tea waste many times with distilled water to eliminate contaminants and coloration following by drying at 105 ºC for 1 hr. Subsequently, it was desiccated at the surrounding temperature and thoroughly powdered. The substrate was then carbonized at 500 °C for 2 hr in an oxygen-restricted environment. The resultant black solid with BET surface area 285.6 m^2/g, TWBC, was cooled to room temperature and utilized as an adsorbent for comparison with commercially available activated carbon under optimal conditions, as shown in Fig. 1.

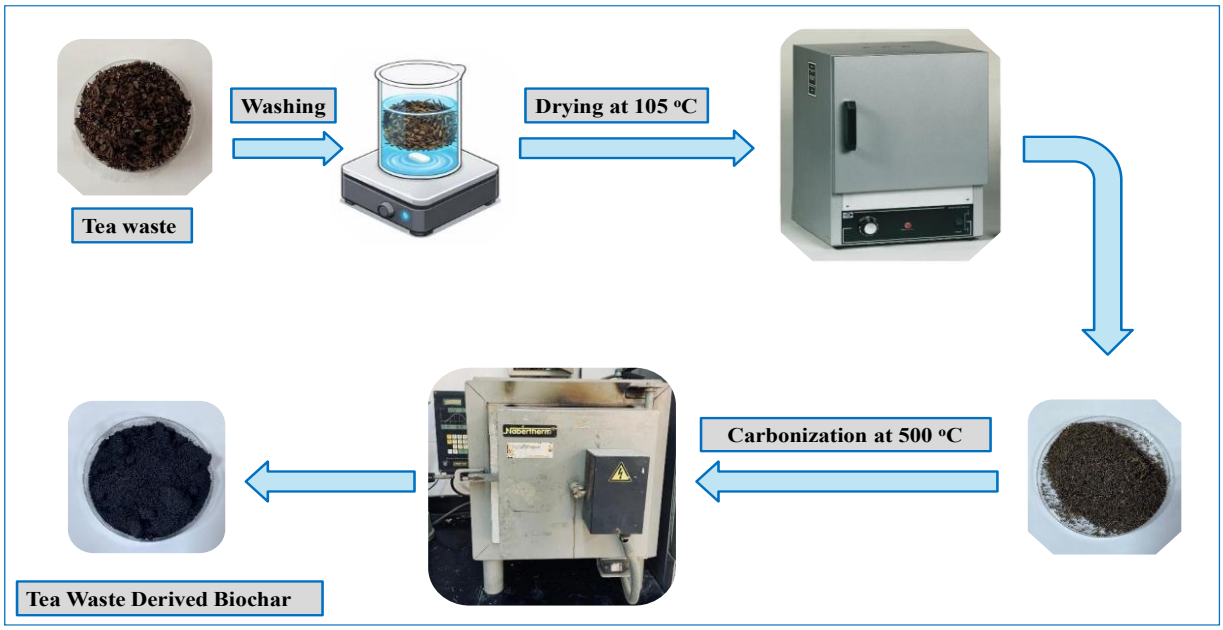

Fig. 1. Tea waste derived biochar preparation

2.2.3. Modified CAC and TWDB with citric acid

The modified CAC and TWDB were synthesized through incorporating citric acid (0.1 M) and heating to 80 °C for 2-3 hr with agitation, followed by washing with distilled water until a pH of 6 -7 was achieved yielding the final adsorbents (CAC-CA and TWDB-CA), which were subsequently dried at 105 °C for 30 min and then used as modified adsorbents for comparison with raw CAC and TWDB under optimal conditions.

2.3. Characterization of adsorbents

Fourier transform infrared spectroscopy (FTIR) was employed to characterize the surface functional groups of the four different adsorbents before the adsorption procedure. The investigation aimed to identify key functional groups, including the hydroxyl (–OH), and the carboxyl (–COOH) groups, anticipated to operate as the primary active sites for Pb (II) ions binding through processes.

2.4. Batch adsorption experiments

The standard stock solution of lead ions (II) 1000 ppm was prepared by dissolving 1.598 g of Pb $(NO_3)_2$ from Merck in 1 L of distilled water and kept in a refrigerator at 4 ºC to inhibit microbial growth and to ensure the stability of Pb in the aqueous solution.

At the first stage number of batch experiments were carried out to investigate the optimal conditions for adsorption lead ions (II) from aqueous solution by utilizing CAC. Adsorption experiments were performed at room temperature under various initial lead ions (II) concentrations, pH, adsorbent dose, adsorbent particle size, and adsorption time. All adsorption experiments were conducted in batch mode using a mechanical shaker on a GEMMY orbital shaker model: VRN-480, operating at a constant shaking rate of 150 rpm to ensure uniform mixing.

The initial concentration range of lead ions (II) was prepared from the stock solution to achieve standard concentrations of 10, 20, 30, 40, 50, and 60 ppm. In order to determine the effects of different pH on adsorption rate, each prepared sample was divided into six 100 mL samples. The pH values of the samples were adjusted to 3, 5, 7, 9, 11, and 13 by using hydrochloric acid (HCl) 0.1 M and sodium hydroxide (NaOH) 1 N solutions. A calibrated digital pH meter was used to measure and monitor the pH at the beginning and end of each adsorption experiment. No external buffering system was employed to avoid interference from competing ions.

A known weight of adsorbent of 0.05, 0.1, 0.15, 0.2, 0.25, and 0.3 g was added to 100 mL of lead nitrate with a

known concentration in a 250 mL glass conical flask. After the addition of adsorbent in each conical flask simultaneously, the content was mixed for 15, 30, 45, 60, 75, and 90 min using a shaker.

After shaking, the conical flasks were removed slowly from the shaker platform, and the contents of the conical flasks were allowed to settle for 5 min. After settlement, the adsorbent was removed by filtration using Whatman filter papers (No. 42) to get a clear supernatant. Then the supernatants were analyzed on an atomic absorption spectrophotometer (AAS) to determine the concentration of lead ions (II) after adsorption.

After determining the optimal conditions for each variable based on the removal efficiency (R %), the variables were fixed, and the following experiments were conducted for each adsorbent (CAC, TWDB, CAC-CA, and TWDB-CA). Subsequently, the remaining Pb (II) concentration was measured after adsorption for each type to determine removal percentage (R %) and equilibrium adsorption capacity (Q_e).

3- Measurements of percentage removal of CAC and lead adsorption capacity of CAC and TWDB pre- and post-modification

According to the concentration of adsorbed pollutant by depositing, the pollutant concentration in the polluted solutions was added from the dissolved pollutant concentration remaining in the solution after adsorption. the removal percentage (R %) was calculated as the following equation:

$$R\ \% = \left[\frac{C_0 - C_{out}}{C_{out}}\right] * 100 \quad (1)$$

To evaluate the equilibrium adsorption capacity (Q_e), expressed in mg/g, represents the amount of lead ions (II) adsorbed per unit mass of adsorbent at equilibrium.

$$Q_e = \left[\frac{C_0 - C_{out}}{m}\right] * \nu \quad (2)$$

Where C_0 and C_{out} represent the concentration of pollutant before and after adsorption process, respectively (ppm each), and ν is the volume of the synthetic aqueous solution (L) and m is the mass of the adsorbent material (g). This metric provides an additional insight into the performance of adsorbents materials. The adsorption capacity reflects the fundamental ability of the adsorbent to capture pb (II) ions and acts as an objective standard to evaluate and compare the efficiency of various adsorbents materials.

4- Adsorption isotherm models

The adsorption capacity of CAC for various concentrations of lead ions (II) (10-60 ppm) was evaluated under operational conditions (Contact time of 30 min, pH of 7, adsorbent dose of 0.2 g/ 100 mL, adsorbent particle size 75-100 mm, and constant shaking rate 150 rpm) at room temperature. The adsorption performance at equilibrium was analyzed by fitting the experimental data to the widely used Langmuir, Freundlich and Temkin isotherm models.

The Langmuir equation is expressed in the following forms [21]:

$$Q_e = \frac{Q_{max} K_L C_e}{1 + K_L C_e} \quad (3)$$

$$\frac{C_e}{Q_e} = \frac{1}{Q_{max} K_L} + \frac{C_e}{Q_{max}} \quad (4)$$

Where Q_e represents adsorption capacity at equilibrium (mg/g), C_e represents lead concentration at equilibrium (ppm), Q_{max} represents maximum adsorption capacity (mg/g), and K_L is Langmuir constant.

The form of Freundlich equation can be expressed as follows [22]:

$$Q_e = K_F C_e^{\frac{1}{n}} \quad (5)$$

$$\ln Q_e = \ln K_F + \frac{1}{n} \ln C_e \quad (6)$$

Where K_F is known as the Freundlich constant which represents the calculated capacity of adsorption, and n is the intensity value for adsorption which determines adsorption type.

The Temkin isotherm model equation can be written as follows [23]:

$$Q_e = B\ \ln K_T + B\ ln C_e \quad (7)$$

5- Adsorption kinetic models

To determine the equilibrium time for the adsorptive removal of lead, with a concentration of 10 ppm of metal solution. The 0.3 g/ 100 mL dose of CAC with particle size of 75 mm, and pH of 5 were used. following adding CAC, the flasks were kept in a shaking incubator at 150 rpm at room temperature. The adsorption capacity was assessed at time intervals of 15, 30, 45, 60, 75, and 90 minutes.

The adsorption kinetics of lead was analyzed using pseudo-first-order, and pseudo-second-order kinetic models by plotting adsorption capacity against time.

The pseudo-first-order equation (PFO) is given below [21]:

$$\ln(Q_e - Q_t) = ln\ Q_e - K_1 t \quad (8)$$

The pseudo-second-order (PSO) equation is given bellow [24]:

$$\frac{t}{Q_t} = \frac{1}{K_2 Q_e^2} + \frac{1}{Q_e} t \quad (9)$$

In this equation, Q_t represents the adsorption capacity of lead (mg/g), at given time (t), Q_e denotes the adsorption capacity (mg/g) at equilibrium, k_1 (min^{-1}) is rate constant of pseudo-first-order equation. And k_2 ($kg/g^{-1}.min^{-1}$) is rate constant for the pseudo-second-order equation.

6- Results

6.1. Effect of initial lead ions (II) concentration and adsorption isotherm models

The influence of initial lead ions (II) concentration was conducted by verifying it (10, 20, 30, 40, 50, and 60 ppm each) keeping adsorbent dosage of 0.2 g/100 mL with particle size 75-100 µm, PH of 7, and adsorption time of 30 min with constant shaking rate 150 rpm at room temperature, on the removal percentage and adsorption capacity of CAC is shown in Fig. 2. The findings indicate that as the concentrations of lead increased, the removal percentage of lead decreased. The maximum removal and of 63 % at the lowest lead concentration of 10 ppm. This behavior reflects the saturation of the limited active sites on the CAC surface at trace concentrations, a higher percentage of available ions can be removed, but as concentration increases, competition for binding active sites intensifies, decreasing R % while increasing the absolute amount of pb (II0 ions adsorbed per unit mass of adsorbent [25]. To explain the adsorption mechanism and surface characteristics, the equilibrium data were analyzed using isotherm models for example Langmuir, Freundlich, and Temkin (Fig. 3, Fig. 4, and Fig. 5). The adsorption isotherm analysis indicated that Langmuir model was the most suitable for lead Fig. 3 and Table 1. The values of optimal adsorption capacities obtained from this model were close to the values obtained from the experimental data. The highest adsorption capacities predicted by the Langmuir model were 12.674 and 10 mg/g, respectively.

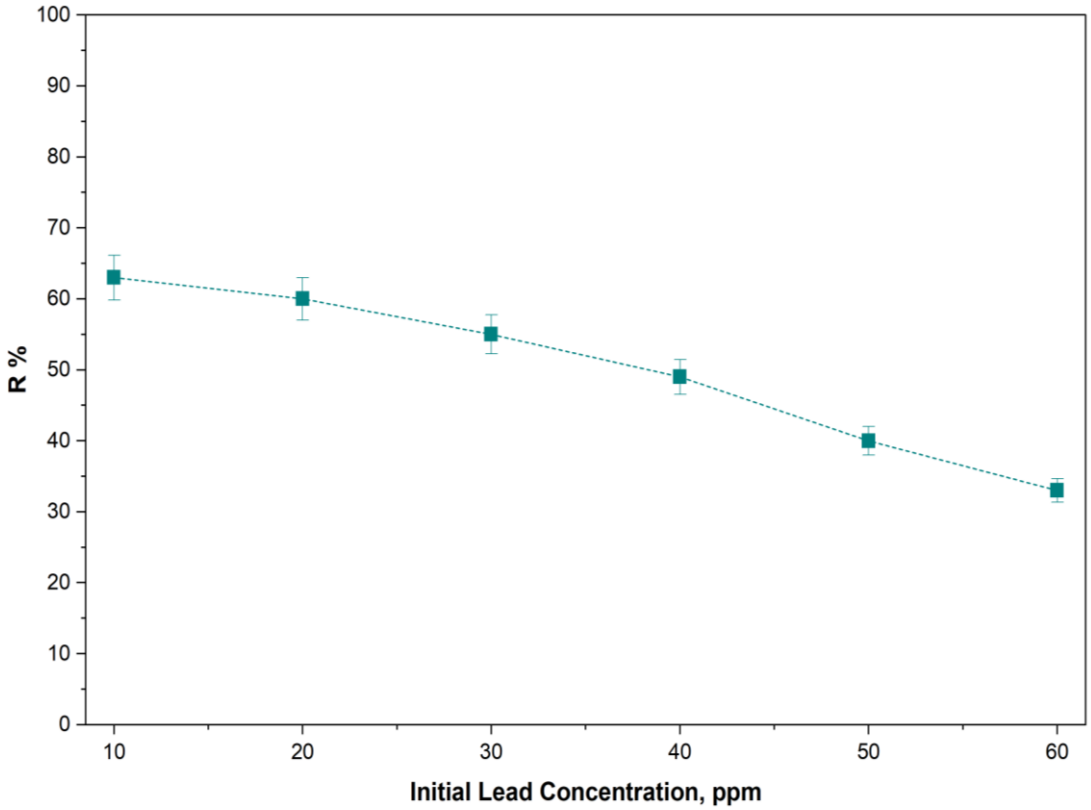

Fig. 2. The effect of initial lead concentration on removal %

Table 1. Parameters of adsorption isotherm models

Langmuir		
K_L	**Q_{max}**	**R^2**
0.115	12.674	97.91 %
Freundlich		
K_F	**n**	**R^2**
1.976	2.051	88.97 %
Temkin		
K_T	**B**	**R^2**
0.903	3.047	93.75 %

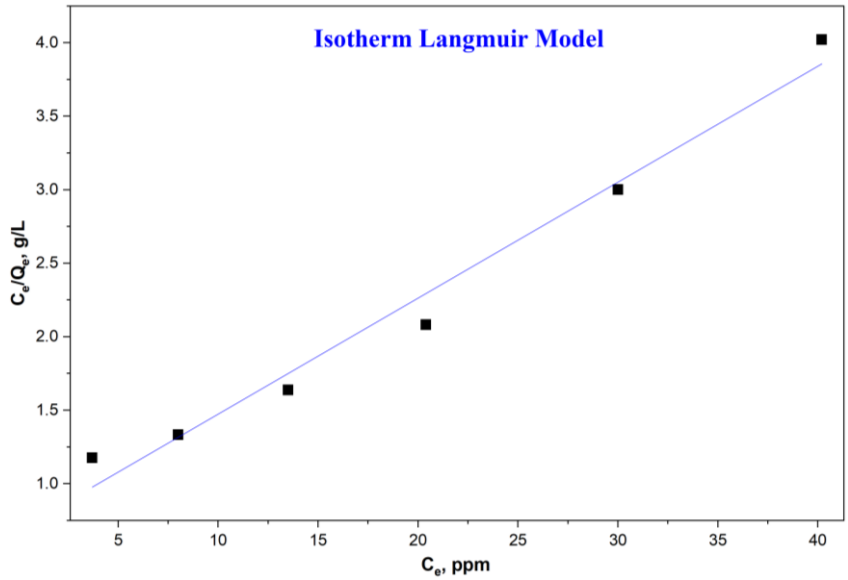

Fig. 3. Langmuir isotherm model

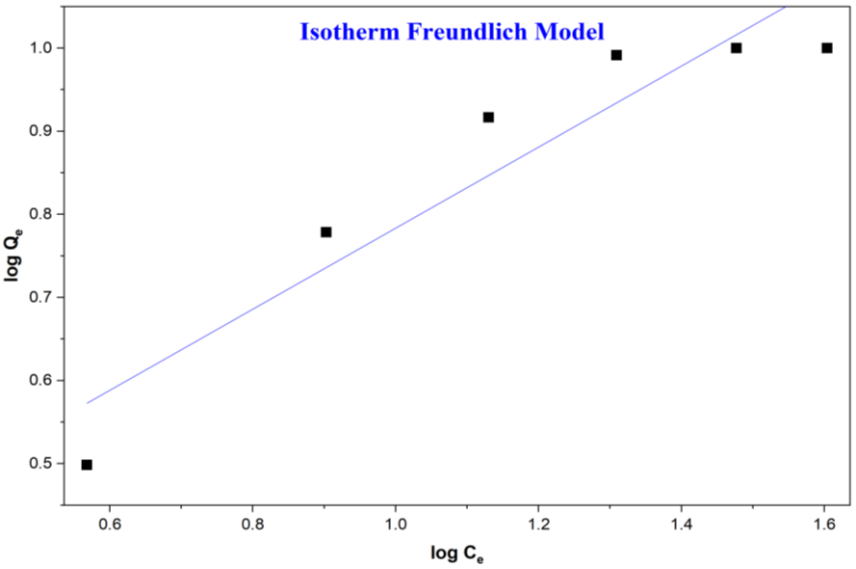

Fig. 4. Freundlich isotherm model

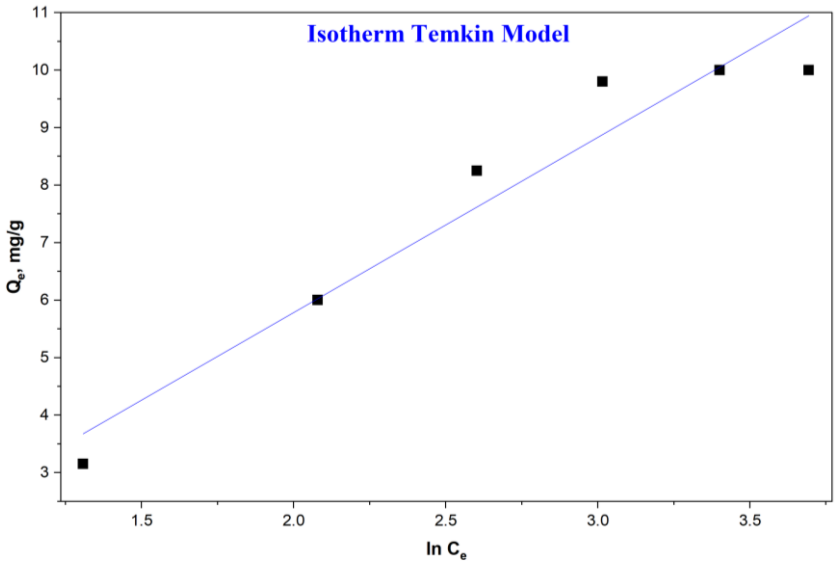

Fig. 5. Temkin isotherm model

6.2. The effect of pH levels on removal %

The effect of pH of solution (3 – 13) on the removal % and adsorption capacity of CAC for lead 10 ppm each, keeping the other parameter constant was shown in Fig. 6. It was noticed that when pH increased from 3 to 5 lead to increase the Removal % from 50 to 66 %. However, pH above 5 resulted in a decline in the Removal %. The reduction in R % beyond pH 5 is due to the formation of soluble hydroxyl complexes ($Pb(OH)^+$, $Pb(OH)_2$) and the precipitation of $Pb(OH)_2$ at pH > 6, which diminishes the availability of free Pb (II) ions for adsorption [26, 27]. These observations match the point of zero charge of CAC, generally between 4 and 6, where optimal surface charge formation facilitates cationic metal ion adsorption [27, 28]. The results highlight the essential role of pH regulation in lead adsorption processes using CAC.

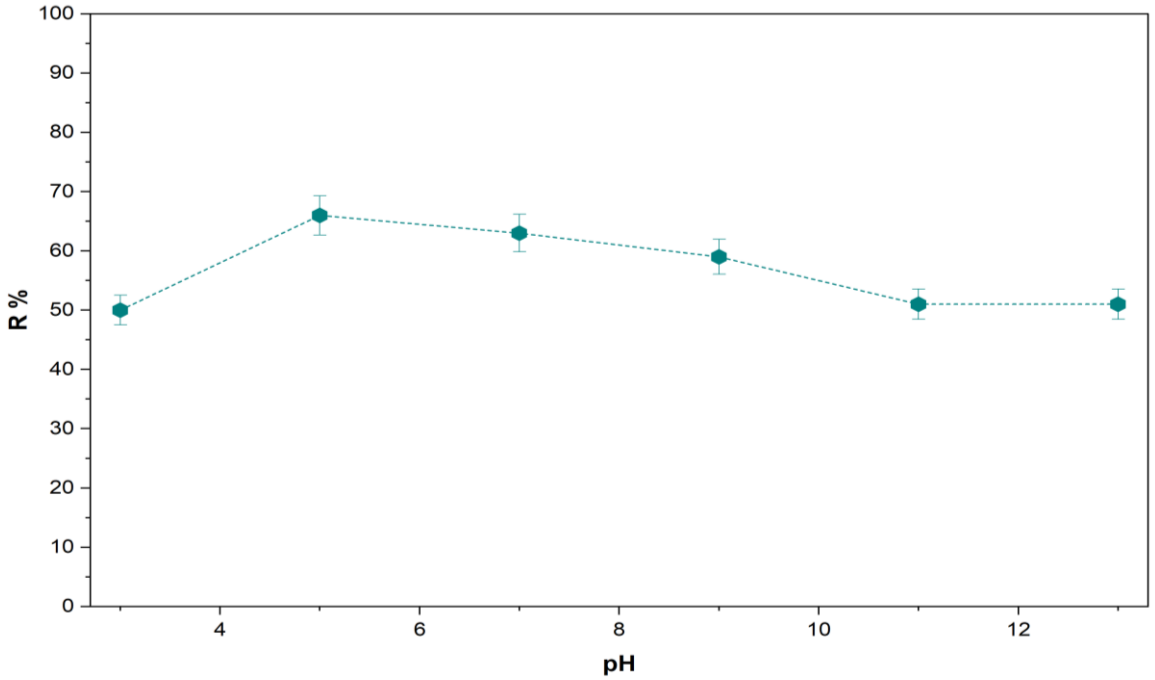

Fig. 6. The effect of pH of solution on removal %

6.3. The effect of CAC dosage and particle size on removal %

The adsorbent dosage is a very critical parameter in batch adsorption systems. The influence of adsorbent dosage (0.05 – 0.3 g / 100 mL) and particle size (≥75, 75 –100, and 100 –125 µm) on lead ions (II) removal was extensively studied. The results indicated that R% increased from 39 – 65 % at the lowest dosage (0.05 g) to 56 – 88 % at the highest dosage (0.3 g) Fig. 7.

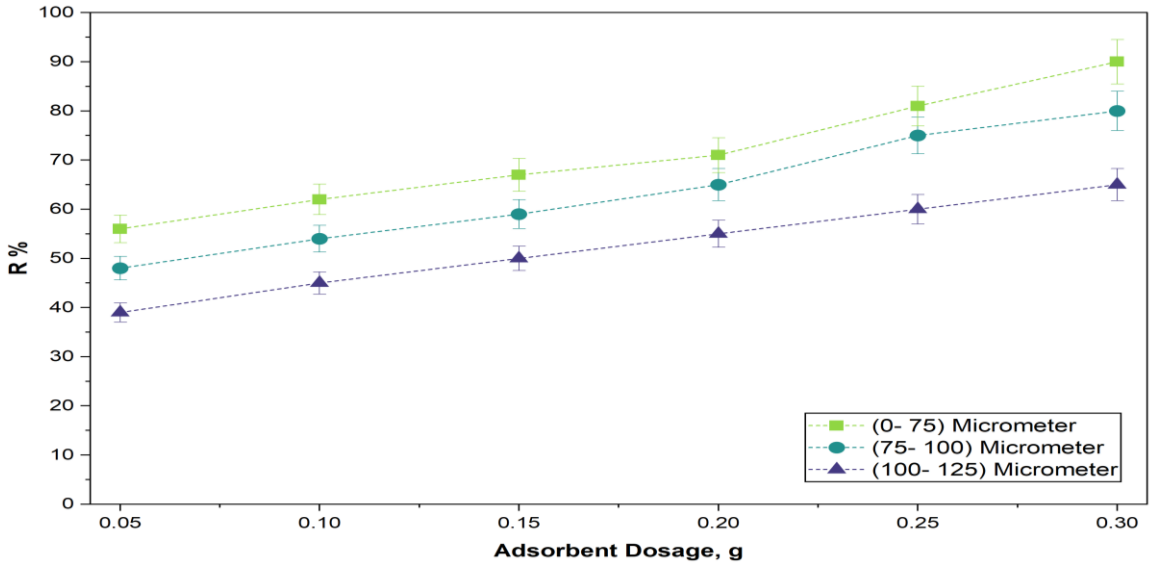

Fig. 7. The effect of CAC dosage and particle size on removal %

The increased R % associated with a greater adsorbent dose is due to the presence of more of active sites on the surface of CAC adsorbent. Increased adsorbent dosage supplies more surface area and more additional sites for lead ions (II) to adhere, resulting in a higher removal from the pollutant water.

The greater performance of fine particle sizes can be attributed to their increased specific surface area and reduced diffusion route length. Smaller particles (≥ 75µm) possess a greater surface area to volume ratio, simplifying enhanced interaction with pb (II). The reduced distance that pb (II) must traverse between particles facilitates their movement from the bulk solution to the adsorption active sites, hence accelerating both the rate and quantity of adsorption. In contrast, higher particle size (100 –125 µm) has decreased the surface area and extended the diffusion pathways, rendering them less efficient in adsorption and slowing the adsorption process. These findings align with literature demonstrating that particle size significantly influences the pb adsorption efficiency, with smaller particles regularly outstripping coarser materials. The optimal dosage for pb (II) ions removal involved utilizing a maximum quantity of adsorbent (0.3 g) and a finer particle size (≥75 µm). This indicates that both parameters must be concurrently adjusted for optimal results in water treatment.

6.4. Effect of adsorption time of lead onto CAC and kinetic models

To investigate the kinetic behavior of lead (II) adsorption onto CAC, the influence of adsorption time (15 – 90 min) was analyzed while maintaining the optimal conditions established in prior experiments (initial lead ions (II) concentration of 10 ppm, pH 5, adsorbent dosage of 0.3 g/100 mL with particle size of ≥75 µm, and keeping shaking rate of 150 rpm). The results of the experiment showed that both R % increased over time. For example, removal efficiency went from 69 % at 15 min to 88 % at 75 min, and then stayed stable at 90 min Fig. 8. This means that adsorption equilibrium was reached at about 75 min.

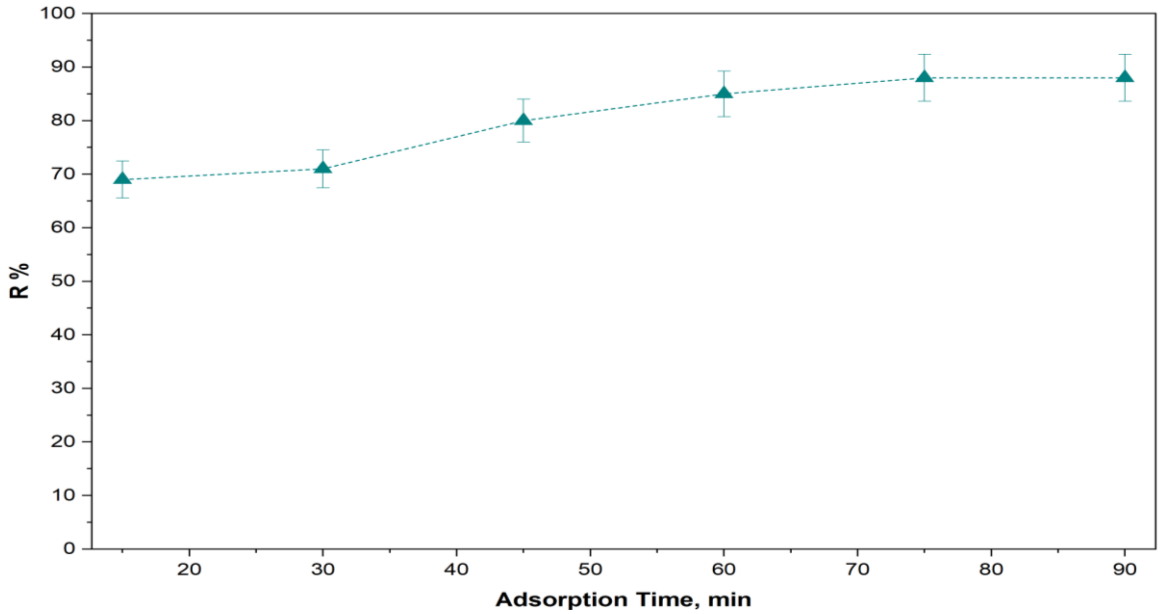

Fig. 8. The effect of adsorption time on removal %

We used PFO and PSO kinetic models to figure out the mechanisms that control the rate of adsorption (Fig. 9, and Fig. 10). The experimentally obtained Qe (3.0 mg/g) was in close agreement with the Pseudo-Second-Order kinetic model prediction (3.21 mg/g), with a deviation of only 6.5%, indicating that the adsorption process is well-described by this model as shown in Fig. 10 and Table 2, which means that chemisorption controls the rate limiting step of lead adsorption. This is because the rate of adsorption is proportional to the square of the number of unoccupied active sites on the adsorbent surface. This behavior indicates that chemical bonding interactions between lead ions and the activated carbon surface drive the adsorption process, rather than mere physisorption [29].

The biphasic kinetic behavior evident in the experimental data can be elucidated by the sequential functioning of two mass transfer mechanisms. During the first quick phase (15 – 45 min), lead (II) moves from the bulk solution to the adsorbent surface through external diffusion (film diffusion). This happens quickly because there are a big concentration gradient and a strong driving force. When the external surface sites become more and more full, the rate-limiting step changes to intraparticle diffusion. This is when pb (II) ions have to move through the pores of commercial activated carbon to reach the internal adsorption active sites. This is what causes the slower equilibration phase (45 – 90 min). The attainment of adsorption equilibrium at 75 min signifies that the system has reached saturation of available active sites under the experimental conditions, beyond which no substantial enhancement in pb (II) ions removal transpires

despite extended contact duration [30]. The quick attainment of equilibrium (75 min) and the strong fit to the PSO kinetic model show how well CAC works to remove pb (II) ions. They also show that the material has a good pore structure and surface characteristics for pb (II) ions transport and chemisorption [30]. These findings show how important it is to optimize the adsorption time in batch adsorption system. They also give quantitative kinetic parameters that can be utilized to design and scale up processes for removing pb (II) ions.

Table 2. Parameters of adsorption kinetic models

Pseudo – 1st Order		
K_1	**Q_e**	**R^2**
0.037	1.57	93.5 %
Pseudo – 2nd Order		
K_2	**Q_e**	**R^2**
0.036	3.21	99.5 %

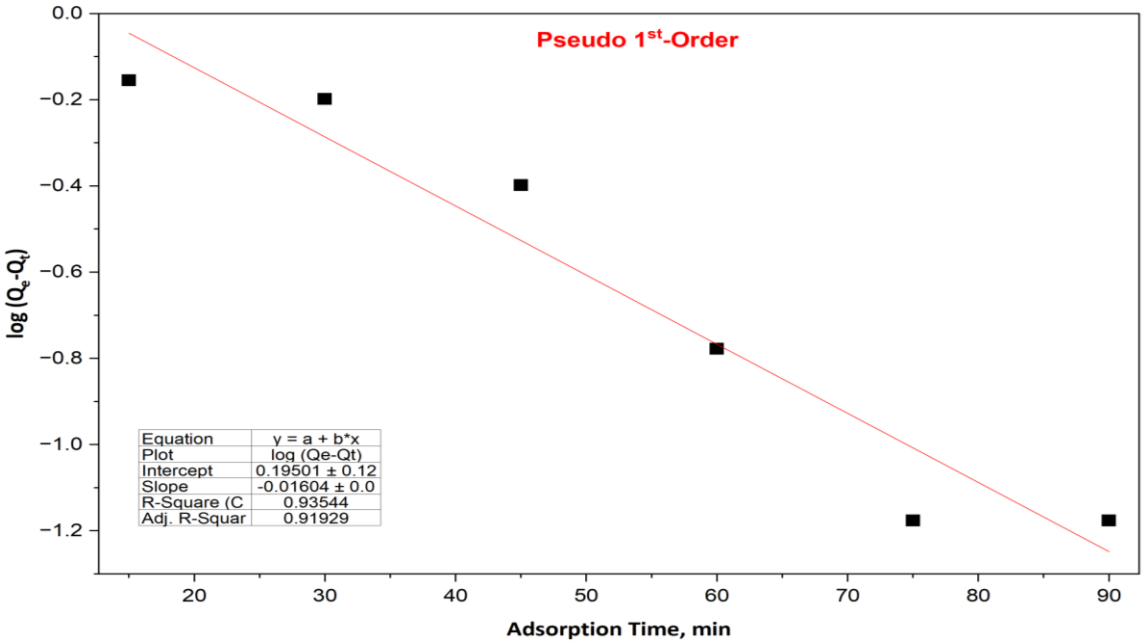

Fig. 9. The pseudo-first-order kinetic model

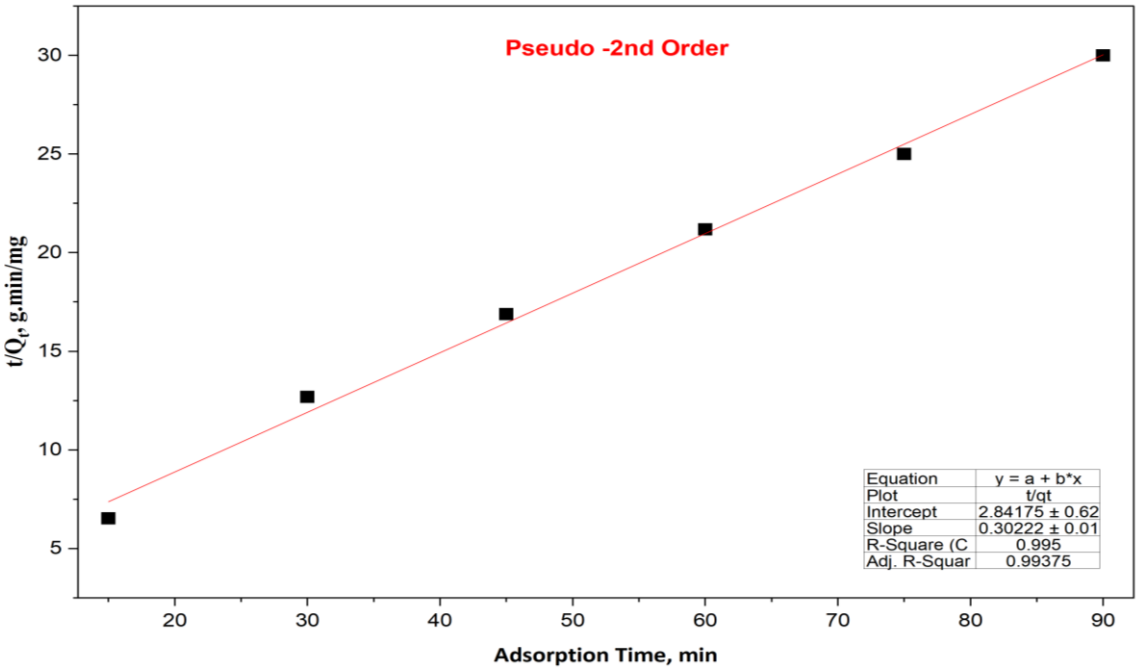

Fig. 10. The pseudo-second-order kinetic model

6.5. Optimization of adsorption parameters

The optimization experiments showed that the maximum R% of pb (II) ions by CAC was achieved under the optimal variables summarized in Table 3. These variables were subsequently adopted as the standard conditions for the comparative study to ensure a fair and controlled evaluation of all different four adsorbents.

Table 3. Optimization adsorption parameters for lead ions (II) removal

Parameter	Unit	Value
Initial Lead Ions (II) Concentration	ppm	10
pH	-	5
Adsorbent Dosage	g	0.3
Adsorbent Particle Size	µm	≥ 75
Adsorption Time	min	75

6.6. Characteristics of adsorbents

The FTIR spectra of CAC and TWDB before and after modification by CA reveal distinct surface functional group distributions that directly provide the reflection of their chemical composition and modification Fig. 11 and Fig. 12. CAC exhibits a relatively simple surface chemistry profile, characterized by a weak, a moderately intense C=O band at 1640 cm^{-1} corresponding to quinone type carbonyl structures and broad –OH stretching band at about 3450 cm^{-1}, with an absent carboxylic acid functionality [31]. In contrast, TWDB provides noticeable wealthier surface chemistry, featuring a sharp and intensified –OH stretching band at about 3450 cm^{-1}, derived from cellulose and lignin components, along with a strong C=O band at about 1635 cm^{-1} and multiple additional absorption features (1419, 1387, 1313, and 1286) cm^{-1} indicative of diverse aromatic and carbonyl structures [32].

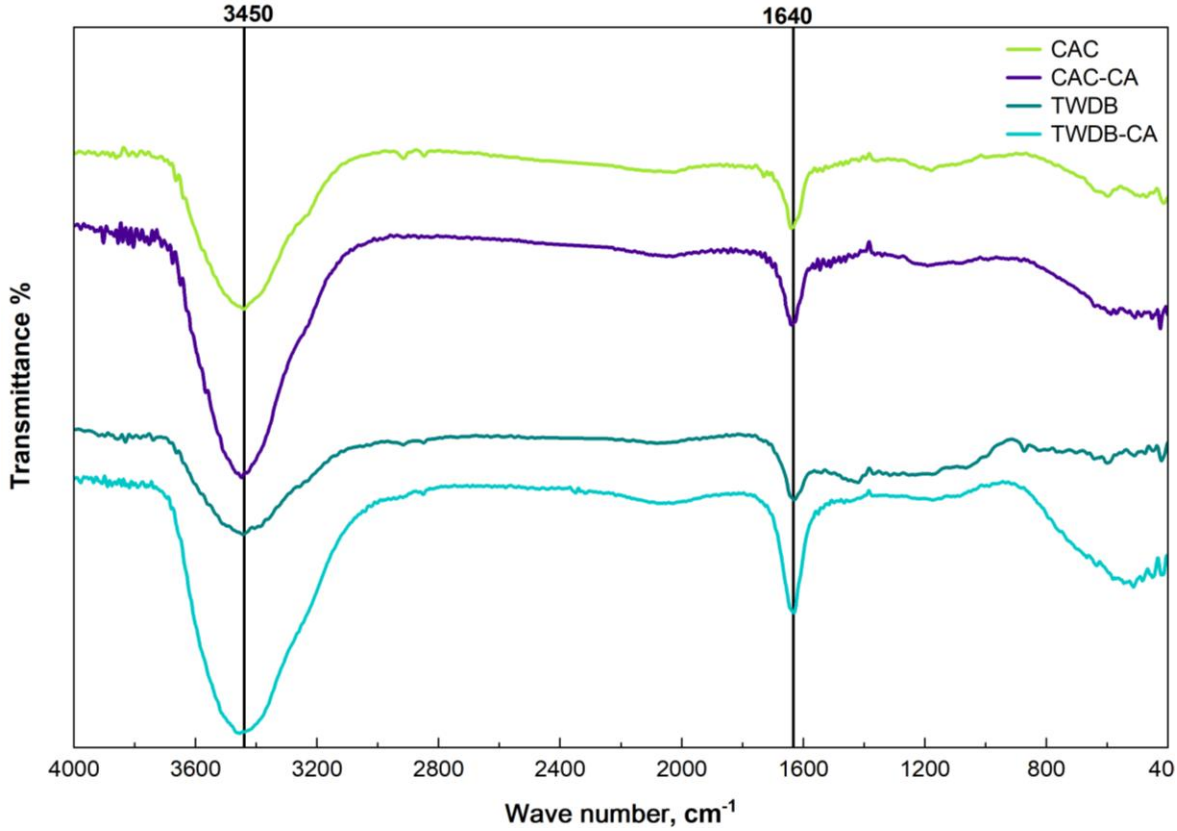

Fig. 11. FTIR spectra of the adsorbents before adsorption

CAC-CA adsorbent material produces an affected transformation in the carbonyl region, introducing a very sharp, intense absorption band at about 1730 cm^{-1} that is the characteristic feature of nonionized carboxylic acid groups, representing successful surface functionalization with carboxylic acid moieties from CA [33]. Simultaneously, the –OH stretching band becomes more pronounced and broader at about 3445 cm^{-1}, indicating enhanced surface polarity and increased hydrogen bonding interactions. TWDB-CA results in the most intense –OH band among all type materials at about 3450 cm^{-1}, demonstrating the cumulative effect of the original biochar abundant hydroxyl groups combined with additional –OH functionality from citric acid, while the carbonyl region shows evidence of carboxylate species (C=O) superimposed on the original carbonyl bands at

about 1630 cm^{-1}, suggesting that CA derived carboxylic groups have been partially ionized on the biochar adsorbent surface [34]. The comparative analysis reveals that modified commercial activated carbon (CAC-CA) uniquely displays the characteristic 1700 cm^{-1} carboxylic acid peak, making it the only material with clearly identifiable free carboxylic acid groups, while TWDB-CA likely contains carboxylate species rather than free carboxylic acids. These FTIR spectra identified functional groups, particularly the newly introduced carboxylic acid to carboxylate groups in the modified adsorbents materials, and the abundant hydroxyl groups in biochar materials form the chemical foundation for metal ion adsorption, with the carboxylic acid groups providing the strongest binding sites according to their higher acidity and resulting ionization at pH values [35].

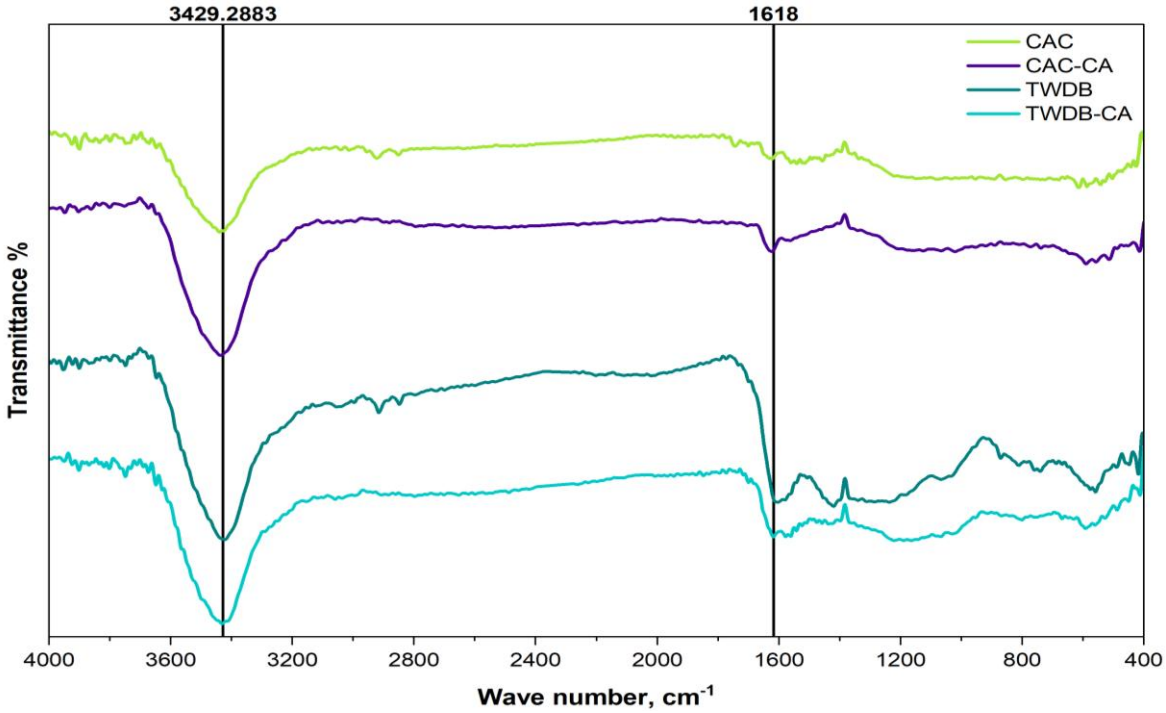

Fig. 12. FTIR spectra of the adsorbents after adsorption

FTIR spectra was analyzed to analyze the surface-active functional groups engaged in the adsorption of Pb (II) ions. Prior to the adsorption process, a broad absorption band about 3450 cm^{-1} was detected, which is attributed to O–H stretching vibrations, indicating the presence of hydroxyl and carboxylic functional groups. Following the adsorption of Pb (II) ions Fig. 12, a notable shift in this band to about 3429 cm^{-1} was observed, accompanied by a decrease in intensity. This change suggests that hydroxyl groups may play an important role in coordination interactions with Pb (II) ions.

Similarly, the band at about 1635 cm^{-1}, attributed to C=O stretching of carboxyl groups and/or aromatic C=C structures, shifted to 1618 cm^{-1} following adsorption. This shift indicates strong interaction between Pb (II) ions and O containing functional groups, particularly deprotonated carboxylate (–COO) sites, supporting the formation of inner sphere surface complexes (pb-O) bonds.

More pronounced spectral changes in the modified samples (CAC-CA and TWDB-CA) confirm that surface modification enhanced the density of active oxygenated groups, thereby improving pb (II) ions binding capacity.

Overall, the observed band shifts in the O–H and C=O regions demonstrate that pb (II) adsorption occurs predominantly by chemisorption through surface complexation and electrostatic attraction more than purely physical-interactions.

6.7. Comparative adsorption study

The experimental results Fig. 13 and Fig. 14, conducted under optimal batch conditions (pH 5, adsorption time 75 min, adsorbent dosage 0.3 g, particle size 75 µm), and shaking rate of 150 rpm at room temperature, clearly demonstrated the effectiveness of citric acid modification in enhancing the removal of lead (II) ions from aqueous solutions by adsorption. Comparative analysis revealed significant improvements in both the removal efficiency % and adsorption capacity of both CAC and TWDB.

Specifically, the modification of CAC-CA increased the equilibrium adsorption capacity from about 2.9 to about 3.17 mg/g and the removal efficiency from about 88% to about 95%. During a greater enhancement was noticed for the adsorbent extracted from waste, the equilibrium adsorption capacity of TWDB increased from 3.329 to 3.333 mg/g, and R % increased from about 90 % to approximately 98 % for TWDB-CA. This notable improvement is mechanically attributed to the successful grafting of oxygen including active functional groups, particularly carboxylic groups (–COOH) and hydroxyl groups (–OH), onto the CAC surfaces [36]. These active

functional groups act as highly active sites, trapping pb (II) ions through strong electrostatic interactions and the formation of surface complexes, thus shifting the dominant removal mechanism from physical adsorption to a stronger and more effective chemisorption process [37,38]. Achieving these high efficiencies under optimal batch conditions underscores the massive potential of these engineered adsorbents.

Notably, the performance of TWDB and TWDB-CA is better than CAC and CAC-CA, highlighting a successful waste-using strategy aligned with circular economy principles [39]. This not only offers a cost-effective and sustainable alternative to expensive commercial absorbents but also has reflective implications for process chemical engineering, enabling the design of more compact and efficient packed layer systems with longer operating cycles for industrial-scale water treatment.

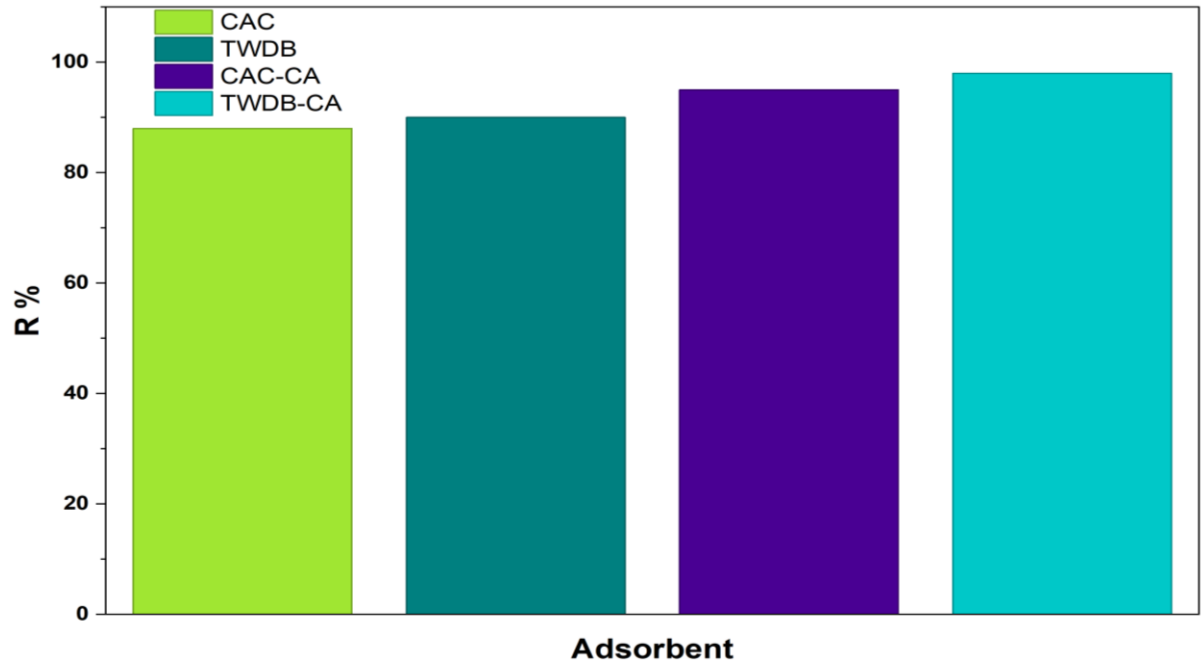

Fig. 13. Efficiency of lead (II) removal at optimal conditions using four different adsorbents

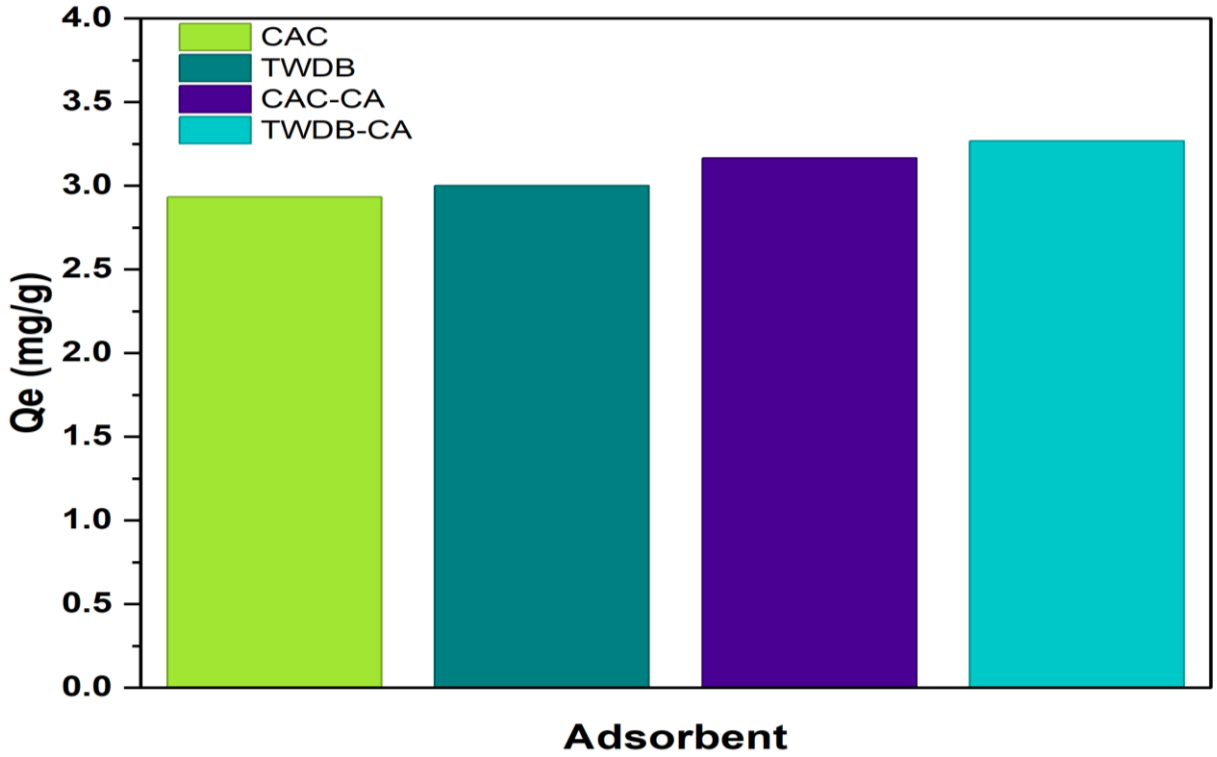

Fig. 14. Equilibrium adsorption capacity at optimal conditions using four different adsorbents

The adsorption capacity of CAC, CAC-CA, TWDB, and TWDB-CA for Pb (II) was determined to be 3.06, 3.331, 3.329, and 3.333 mg/g respectively. Previous studies have confirmed that PM exhibits a higher adsorption capacity compared to many other plants based biosorbents [40-42]. A comparative analysis of maximum adsorption capacities for Pb using various biosorbents from previous studies is presented in Table 4.

Table 4. Comparison of pb adsorption capacity of various biosorbents from previous studies [43-46]

Type of Biosorbent	Adsorption capacity (mg/g)	Reference
Coffee-Pulp	24.10	[43]
Maize-Cop	14.60	[44]
Sawdust	15.90	[45]
Shrimp Shell Waste	15.32	[46]

7- Conclusion

This study successfully established the optimal experimental variables for the adsorption process utilizing CAC. The investigation into the adsorption mechanism revealed that the equilibrium data were best represented by the Langmuir isotherm model, which suggests a mono-layer adsorption process onto a homogeneous surface. Furthermore, the adsorption kinetics were better described by the PSO model with R^2 = 99.5 % compared to the PFO model, indicating that chemisorption is the rate controlling step.

The FTIR analysis showed that the CA-CA and TWDB-CA substantially increased the density of active functional groups (⁻OH) and (C=O) on adsorbent surface. This oxygen containing active functional groups serve as primary active sites for binding, thereby augmenting the overall adsorption capacity. In summary, this work provides a viable and sustainable approach for enhancing efficient adsorbents from waste biomass for environmental remediation applications.

A key contribution of this research is the comparative performance evaluation of different adsorbents materials. The results demonstrated that the adsorption efficiency of TWDB and TWDB-CA was significantly enhanced to a level equivalent to that of CAC. These findings underscore the potential of valorizing agricultural waste into a high-performance, cost-effective adsorbent material.

Acknowledgments

The author expresses appreciation to the Department of Chemical Engineering at the College of Engineering, University of Baghdad and the Department of Applied Chemistry at the College of Applied Sciences, University of Technology for their assistance, support, and supplying laboratory facilities.

References

[1] M. Jaishankar, T. Tseten, N. Anbalagan, B. B. Mathew, and K. N. Beeregowda, "Toxicity, mechanism and health effects of some heavy metals," *Interdisciplinary Toxicology*, vol. 7, no. 2, pp. 60–72, Jun. 2014, https://doi.org/10.2478/intox-2014-0009

[2] World Health Organization, Guidelines for Drinking-water Quality, 4th ed., Geneva, Switzerland: WHO Press, 2017 (updated 2022).

[3] United States Environmental Protection Agency, "Lead and Copper Rule," *Washington*, DC, USA, 2022.

[4] I. R. Chowdhury, S. Chowdhury, M. A. J. Mazumder, and A. Al-Ahmed, "Removal of lead ions (Pb^{2+}) from water and wastewater: a review on the low-cost adsorbents," *Applied Water Science*, vol. 12, no. 8, p. 185, Jun. 2022, https://doi.org/10.1007/s13201-022-01703-6

[5] F. Fu and Q. Wang, "Removal of heavy metal ions from wastewaters: A review," *Journal of Environmental Management*, vol. 92, no. 3, pp. 407–418, Dec. 2011, https://doi.org/10.1016/j.jenvman.2010.11.011

[6] M. Gęca, M. Wiśniewska, and P. Nowicki, "Biochars and activated carbons as adsorbents of inorganic and organic compounds from multicomponent systems – A review," *Advances in Colloid and Interface Science*, vol. 305, p. 102687, May 2022, https://doi.org/10.1016/j.cis.2022.102687

[7] J. Lach and E. Okoniewska, "Equilibrium, Kinetic, and Diffusion Mechanism of lead (II) and cadmium (II) Adsorption onto Commercial Activated Carbons," *Molecules*, vol. 29, no. 11, p. 2418, May 2024, https://doi.org/10.3390/molecules29112418

[8] S. Iijima, "Helical microtubules of graphitic carbon," *Nature*, vol. 354, no. 6348, pp. 56–58, Nov. 1991, https://doi.org/10.1038/354056a0

[9] V. K. Gupta, S. Agarwal, and T. A. Saleh, "Chromium removal by combining the magnetic properties of iron oxide with adsorption properties of carbon nanotubes," *Water Research*, vol. 45, no. 6, pp. 2207–2212, Jan. 2011, https://doi.org/10.1016/j.watres.2011.01.012

[10] M. Karnib, A. Kabbani, H. Holail, and Z. Olama, "Heavy metals removal using activated carbon, silica and silica activated carbon composite," *Energy Procedia*, vol. 50, pp. 113–120, Jan. 2014, https://doi.org/10.1016/j.egypro.2014.06.014

[11] Y. Xu *et al.*, "Study on Efficient adsorption mechanism of PB^{2+} by Magnetic Coconut Biochar," *International Journal of Molecular Sciences*, vol. 23, no. 22, p. 14053, Nov. 2022, https://doi.org/10.3390/ijms232214053

[12] S. H. Khazaal, F. Al-Sheikh, and M. Al-Ameri, "Using activated carbon to adsorb Co (II) from synthetic solution: Isotherms and optimization studies," *AIP Conference Proceedings*, vol. 2670, p. 060017, Jan. 2022, https://doi.org/10.1063/5.0095860

[13] M. H. Ullah and M. J. Rahman, "Adsorptive removal of toxic heavy metals from wastewater using water hyacinth and its biochar: A review," *Heliyon*, vol. 10, no. 17, p. e36869, Aug. 2024, https://doi.org/10.1016/j.heliyon.2024.e36869

[14] S. W. Shakir et al., "Examination and Improvement of the Taguchi-Based Nanofluids Impact on CO_2 Absorption using Al_2O_3 Nanoparticles," *Journal of Advanced Research in Fluid Mechanics and Thermal Sciences*, vol. 120, no. 1, pp. 204–216, Aug. 2024, https://doi.org/10.37934/arfmts.120.1.204216

[15] D. Laishram, S. Kim, S. Lee, and S. Park, "Advancements in Biochar as a sustainable adsorbent for water pollution mitigation," *Advanced Science*, vol. 12, no. 19, p. e2410383, Apr. 2025, https://doi.org/10.1002/advs.202410383

[16] S. H. Dhobi, D. Neupane, S. Koirala, and D. D. Mulmi, "Waste tea as absorbent for removal of heavy metal present in contaminated water," *Heliyon*, vol. 10, no. 21, p. e39519, Oct. 2024, https://doi.org/10.1016/j.heliyon.2024.e39519

[17] M. K. Rajput, R. Hazarika, and D. Sarma, "Zerovalent iron decorated tea waste derived porous biochar [ZVI@TBC] as an efficient adsorbent for Cd(II) and Cr(VI) removal," *Journal of Environmental Chemical Engineering*, vol. 11, no. 4, p. 110279, Jun. 2023, https://doi.org/10.1016/j.jece.2023.110279

[18] Y. Liu, L. Zhang, Z. Zhang, Y. Zhang, and Y. Guan, "Citrate-modified biochar for simultaneous and efficient plant-available silicon release and copper adsorption: Performance and mechanisms," *Journal of Environmental Management*, vol. 301, p. 113819, 2022, https://doi.org/10.1016/j.jenvman.2021.113819

[19] A. Ekanayake, A. U. Rajapaksha, M. Ahmad, and M. Vithanage, "Enhanced Adsorption of Hexavalent Chromium from Aqueous Solution by Citric Acid-Modified Biochar from Invasive Plant Biomass," *Water Air & Soil Pollution*, vol. 234, no. 7, Jul. 2023, https://doi.org/10.1007/s11270-023-06456-9

[20] B. Haider et al., "Adsorptive removal of lead from wastewater using press mud with evaluation of kinetics and adsorption isotherms," *Scientific Reports*, vol. 15, no. 1, p. 22823, Jul. 2025, https://doi.org/10.1038/s41598-025-05169-9

[21] N. Jawad and T. M. Naife, "Mathematical Modeling and Kinetics of Removing Metal Ions from Industrial Wastewater," *Iraqi Journal of Chemical and Petroleum Engineering*, vol. 23, no. 4, pp. 59–69, 2022, https://doi.org/10.31699/IJCPE.2022.4.8

[22] S. M. Al-Jubouri, H. A. Al-Jendeel, S. A. Rashid, and S. Al-Batty, "Green synthesis of porous carbon cross-linked Y zeolite nanocrystals material and its performance for adsorptive removal of a methyl violet dye from water," *Microporous and Mesoporous Materials*, vol. 356, p. 112587, Apr. 2023, https://doi.org/10.1016/j.micromeso.2023.112587

[23] M. S. Abdulrahman, A. A. Alsarayreh, S. K. A. Barno, M. A. Abd Elkawi, and A. S. Abbas, "Activated carbon from sugarcane as an efficient adsorbent for phenol from petroleum refinery wastewater: Equilibrium, kinetic, and thermodynamic study," *Open Engineering,* vol. 13, no. 1, June 2023, https://doi.org/10.1515/eng-2022-0442

[24] T. R. Sahoo and B. Prelot, "Adsorption processes for the removal of contaminants from wastewater: The perspective role of nanomaterials and nanotechnology," *Nanomaterials for the Detection and Removal of Wastewater Pollutants*, 1st ed., Amsterdam, Netherlands: Elsevier Inc., Jun. 2020, https://doi.org/10.1016/B978-0-12-818489-9.00007-4

[25] M. Erdem, S. Ucar, S. Karagöz, and T. Tay, "Removal of Lead (II) Ions from Aqueous Solutions onto Activated Carbon Derived from Waste Biomass," *The Scientific World Journal*, vol. 2013, Article ID 146092, 2013. https://doi.org/10.1155/2013/146092

[26] A. A. Alghamdi, A. B. Al-Odayni, W. S. Saeed, A. Al-Kahtani, F. A. Alharthi, and T. Aouak, "Efficient Adsorption of Lead (II) from Aqueous Phase Solutions Using Polypyrrole-Based Activated Carbon," *Materials (Basel)*, vol. 12, no. 12, p. 2020, Jun. 2019, https://doi.org/10.3390/ma12122020

[27] M. Erdem, S. Ucar, S. Karagöz, and T. Tay, "Removal of Lead (II) Ions from Aqueous Solutions onto Activated Carbon Derived from Waste Biomass," *The Scientific World JOURNAL*, vol. 2013, no. 1, p. 146092, Jan. 2013, https://doi.org/10.1155/2013/146092

[28] A. M. Youssef, A. I. Ahmed, M. I. Amin, and U. A. El-Banna, "Adsorption of lead by activated carbon developed from rice husk," *Desalination and Water Treatment*, vol. 54, no. 6, pp. 1694–1707, May 2015, https://doi.org/10.1080/19443994.2014.896289

[29] M. Erdem, S. Ucar, S. Karagöz, and T. Tay, "Removal of Lead (II) Ions from Aqueous Solutions onto Activated Carbon Derived from Waste Biomass," *The Scientific World Journal*, vol. 2013, Article ID 146092, 2013, https://doi.org/10.1155/2013/146092

[30] J. Lach and E. Okoniewska, "Equilibrium, Kinetic, and Diffusion Mechanism of Lead(II) and Cadmium(II) Adsorption onto Commercial Activated Carbons," *Molecules*, vol. 29, no. 11, p. 2418, May 2024, https://doi.org/10.3390/molecules29112418

[31] J. P. Chen, S. Wu, and K.-H. Chong, "Surface modification of a granular activated carbon by citric acid for enhancement of copper adsorption," *Carbon*, vol. 41, no. 10, pp. 1979–1986, Jan. 2003, https://doi.org/10.1016/S0008-6223(03)00197-0

[32] S. Liu et al., "High-efficiency adsorption of various heavy metals by tea residue biochar loaded with nanoscale zero-valent iron," *Environmental Progress & Sustainable Energy*, vol. 40, no. 6, Jun. 2021, https://doi.org/10.1002/ep.13706

[33] M. Zabiszak, M. Nowak, K. Taras-Goslinska, M. T. Kaczmarek, Z. Hnatejko, and R. Jastrzab, "Carboxyl groups of citric acid in the process of complex formation with bivalent and trivalent metal ions in biological systems," *Journal of Inorganic Biochemistry*, vol. 182, pp. 37–47, Feb. 2018, https://doi.org/10.1016/j.jinorgbio.2018.01.017

[34] R. Janu et al., "Biochar surface functional groups as affected by biomass feedstock, biochar composition and pyrolysis temperature," *Carbon Resources Conversion*, vol. 4, pp. 36–46, Jan. 2021, https://doi.org/10.1016/j.crcon.2021.01.003

[35] Z. Shen, Y. Zhang, F. Jin, O. McMillan, and A. Al-Tabbaa, "Qualitative and quantitative characterization of adsorption mechanisms of lead on four biochars," *The Science of the Total Environment*, vol. 609, pp. 1401–1410, Aug. 2017, https://doi.org/10.1016/j.scitotenv.2017.07.027

[36] U. S. Rashid and A. N. Bezbaruah, "Citric acid modified granular activated carbon for enhanced defluorination," *Chemosphere*, vol. 252, p. 126639, Mar. 2020, https://doi.org/10.1016/j.chemosphere.2020.126639

[37] C.-Y. Kuo, C.-H. Wu, and M.-J. Chen, "Adsorption of lead ions from aqueous solutions by citric acid-modified celluloses," *Desalination and Water Treatment*, vol. 55, no. 5, pp. 1264–1270, 2015, https://doi.org/10.1080/19443994.2014.926460

[38] P. M. Godwin, Y. Pan, H. Xiao, and M. T. Afzal, "Progress in preparation and application of modified biochar for improving heavy metal ion removal from wastewater," *Journal of Bioresources and Bioproducts*, vol. 4, no. 1, pp. 31–42, Feb. 2019, https://doi.org/10.21967/jbb.v4i1.180

[39] A. Tiwari and M. Chinthala, "Tea waste to biochar: A comparative analysis of conventional and microwave-assisted pyrolysis methods," *Journal of Analytical and Applied Pyrolysis*, vol. 192, p. 107320, Aug. 2025, https://doi.org/10.1016/j.jaap.2025.107320

[40] A. Gunjal, "Kinetics study for the removal of heavy metals by the agroindustry by-products," *Proceedings of the Indian National Science Academy*, vol. 87, no. 1, pp. 57–62, Mar. 2021, https://doi.org/10.1007/s43538-021-00005-w

[41] I. M. Raimondi, V. G. S. Rodrigues, J. Z. Lima, J. P. Marques, and L. A. A. Vaz, "The potential use of Pressmud as reactive material for CD2+ removal: adsorption equilibrium, kinetics, desorption, and bioaccessibility," *Water Air & Soil Pollution*, vol. 231, no. 7, Jul. 2020, https://doi.org/10.1007/s11270-020-04746-0

[42] I. M. Raimondi, E. M. Vieira, L. a. A. Vaz, and V. G. S. Rodrigues, "Comparison of sugarcane pressmud with traditional low-cost materials for adsorption of lead and zinc in mining areas," *International Journal of Environmental Science and Technology*, vol. 19, no. 6, pp. 4627–4644, 2022, https://doi.org/10.1007/s13762-021-03420-0

[43] D. L. Gómez-Aguilar, J. P. Rodríguez-Miranda, D. Baracaldo-Guzmán, O. J. Salcedo-Parra, and J. A. Esteban-Muñoz, "Biosorption of PB(II) using coffee pulp as a sustainable alternative for wastewater treatment," *Applied Sciences*, vol. 11, no. 13, p. 6066, Jun. 2021, https://doi.org/10.3390/app11136066

[44] I. Abdelfattah, A. A. Ismail, F. A. Sayed, A. Almedolab, and K. M. Aboelghait, "Biosorption of heavy metals ions in real industrial wastewater using peanut husk as efficient and cost-effective adsorbent," *Environmental Nanotechnology Monitoring & Management*, vol. 6, pp. 176–183, Oct. 2016, https://doi.org/10.1016/j.enmm.2016.10.007

[45] Y. Bulut and Z. Tez, "Removal of heavy metals from aqueous solution by sawdust adsorption," *Journal of Environmental Sciences*, vol. 19, no. 2, pp. 160–166, Feb. 2007, https://doi.org/10.1016/S1001-0742(07)60026-6

[46] S. Boddu, A. Chandra, and A. A. Khan, "Biosorption of Cu(II), Pb(II) from electroplating industry effluents by treated shrimp shell," *Materials Today Proceedings*, vol. 57, pp. 1520–1527, 2022, https://doi.org/10.1016/j.matpr.2021.12.052

تحسين ونمذجة امتزاز أيونات الرصاص الثنائية على الممتزات الكربونية: تقييم المقارنة بين اداء الكربون المنشط التجاري الخام والفحم الحيوي المشتق من مخلفات الشاي قبل وبعد التعديل بحامض الستريك

شيماء حسن خزعل [١، *]

١ قسم الكيمياء التطبيقية، كلية العلوم التطبيقية، الجامعة التكنولوجية، بغداد، العراق

الخلاصة

بحثت هذه المقالة فعالية نسبة إزالة أيونات الرصاص من الماء الاصطناعي في دراسة تجريبية. أُجريت تجارب متعددة لتحديد المتغيرات المثلى لتحقيق أعلى نسبة إزالة باستخدام الكربون المنشط التجاري. شملت معايير العملية الرئيسية المدروسة: التركيز الابتدائي لأيونات الرصاص، درجة الحموضة، وحجم جزيئات المادة الماصة وجرعة المادة الماصة، وزمن الامتصاص.

وقد تحققت أعلى نسبة إزالة عند تركيز ابتدائي لأيونات الرصاص الثنائية قدره ١٠ جزء في المليون، ودرجة حموضة ٥، وجرعة مادة ماصة ٠.٣ غرام بحجم جزيئات ٧٥ ميكرومتر، وزمن تلامس ٧٥ دقيقة. استخدم هذا البحث نماذج متساوية الحرارة لتحديد كيفية وصول النظام إلى حالة الاستقرار. وقد أكد نموذج لانغمويير أعلى دقة، كما يتضح من النتائج بمعامل ارتباط (R^2) يبلغ حوالي ٩٧.٩١٪. وُصفت البيانات الحركية بدقة عالية باستخدام نموذج التفاعل من الرتبة الثانية الزائفة، مما يشير إلى أن الامتزاز الكيميائي هو العامل المحدد لمعدل التفاعل، وهو ما أكدته قيمة معامل الارتباط البالغة ٩٩.٥٪. دُرست أربع مواد ماصة لتقييم فعاليتها في إزالة أيونات الرصاص (II): الكربون المنشط (CAC)، والفحم الحيوي المشتق من مخلفات الشاي (TWDB)، والكربون المنشط والفحم الحيوي المشتق من مخلفات الشاي المعدلين بحمض الستريك (CA). أظهرت الدراسة أن هذه المواد الماصة، بالإضافة إلى المادة المعدلة، فعالة وغير مكلفة، ويمكن استخدام المخلفات الزراعية كطريقة فعالة لإزالة أيونات الرصاص (II) من المياه الملوثة.

الكلمات الدالة: إزالة أيونات الرصاص (II)، الامتزاز، الكربون المنشط التجاري، متساويات الحرارة والحركية، الفحم الحيوي المشتق من مخلفات الشاي، تعديل حمض الستريك.